NeuroImage: Clinical 36 (2022) 103249

Contents lists available at ScienceDirect

NeuroImage: Clinical

journal homepage: www.elsevier.com/locate/ynicl

Structural alterations of the insula in depression patients – A 7-Tesla-MRI study

Gereon J. Schnellbächer [a], Ravichandran Rajkumar [a,b,c], Tanja Veselinović [a,b,1], Shukti Ramkiran [a,b], Jana Hagen [a], N. Jon Shah [b,c,d,e], Irene Neuner [a,b,c,*,1]

[a] Department of Psychiatry, Psychotherapy and Psychosomatics, RWTH Aachen University, 52074 Aachen, Germany
[b] Institute of Neuroscience and Medicine 4, INM-4, Forschungszentrum Jülich, Germany
[c] JARA-BRAIN, 52074 Aachen, Germany
[d] Department of Neurology, RWTH Aachen University, 52074 Aachen, Germany
[e] Institute of Neuroscience and Medicine 11, INM-11, Forschungszentrum Jülich, Germany

ARTICLE INFO

Keywords:
Insular cortex
Major depressive disease
7T-Tesla MRI, subfield analysis

ABSTRACT

Introduction: The insular cortex is part of a network of highly connected cerebral "rich club" - regions and has been implicated in the pathophysiology of various psychiatric and neurological disorders, of which major depressive disease is one of the most prevalent. "Rich club" vulnerability can be a contributing factor in disease development. High-resolution structural subfield analysis of insular volume in combination with cortical thickness measurements and psychological testing might elucidate the way in which the insula is changed in depression.

Material and methods: High-resolution structural images of the brain were acquired using a 7*T*-MRI scanner. The mean grey matter volume and cortical thickness within the insular subfields were analysed using voxel-based morphometry (VBM) and surface analysis techniques respectively. Insular subfields were defined according to the Brainnetome Atlas for VBM - and the Destrieux-Atlas for cortical thickness - analysis. Thirty-three patients with confirmed major depressive disease, as well as thirty-one healthy controls matched for age and gender, were measured. The severity of depression in MDD patients was measured via a BDI-II score and objective clinical assessment (AMDP). Intergroup statistical analysis was performed using ANCOVA. An intragroup multivariate regression analysis of patient psychological test results was calculated. Corrections for multiple comparisons was performed using FDR.

Results: Significant differences between groups were observed in the left granular dorsal insula according to VBM-analysis. AMDP-scores positively correlated with cortical thickness in the right superior segment of the circular insular sulcus.

Conclusions: The combination of differences in grey matter volume between healthy controls and patients with a positive correlation of cortical thickness with disease severity underscores the insula's role in the pathogeneses of MDD. The connectivity hub insular cortex seems vulnerable to disruption in context of affective disease.

1. Introduction

Major depressive disorder (MDD) is a debilitating disorder that has been suggested to be the leading cause of disability worldwide (Friedrich, 2017). It is a complex illness with varying phenotypes and intensities. There is a high public interest in better understanding the underlying processes, but many questions still remain. Based on resting-state functional connectivity, Drysdale et al. (2017) identified four different biotypes of depression marked by varying patterns of disruption in functional connectivity. Several cortical structures were found to be associated with all four biotypes, indicating their importance for pathophysiology. Among the most prominent of these was the insular

Abbreviations: AMDP, Arbeitsgemeinschaft für Methodik und Dokumentation in der Psychiatrie; ANCOVA, analysis of covariance; BDI-II, Beck Depression Inventory 2; FDR, false-discovery rate; GMV, grey matter volume; MDD, major depressive disease; TIV, total intracranial volume; VBM, voxel based morphology.

* Corresponding author.
E-mail address: ineuner@ukaachen.de (I. Neuner).

[1] These authors contributed equally to this work.

https://doi.org/10.1016/j.nicl.2022.103249
Received 14 March 2022; Received in revised form 26 September 2022; Accepted 23 October 2022
Available online 27 October 2022

cortex.

The insula is an extensively connected hub region integrating various sensory modalities and cognitive functions (Seeley et al., 2007). On a microscopic level, three different parts have long been identified, namely the granular (posterior), agranular (anterior) and dysgranular (intermediate) insula (Mesulam and Mufson, 1982; Benarroch, 2019). Similarly, a functional connectivity analysis revealed three subregions. A ventral anterior part of the insula converged with the pregenual anterior cingulate cortex, the dorsal anterior insula coactivated with the dorsal anterior cingulate cortex, and the posterior insula connected to primary and secondary somatomotor cortices (Deen et al., 2011). Behavioural analysis of a tripartite insula division has suggested a certain degree of specificity for the domains of emotion and chemosensation in the ventroanterior part, cognition and executive control in the dorsoanterior and a somatosensory and sensorimotor emphasis in the posterior part (Chang et al., 2013). A meta-analysis by Kurth et al. (2010a), Kurth et al. (2010b) came to similar conclusions with the delineation of a sensorimotor, socioemotional, cognitive and olfactory-gustatory area within the insula. The partitioning of the insula both structurally and functionally is thus well replicated. However, strict segregation might not adequately reflect the insula's integrative role in multimodal information (Almashaikhi et al., 2014; Gogolla, 2017), and network analysis has highlighted the overlap in connectivity between subdivisions while also emphasizing the particularly high degree of interconnectivity of the dorsal anterior insula (Uddin et al., 2014).

Functional and structural alterations associated with the insular cortex are related to a spectrum of diseases, including depression (Takahashi et al., 2010; Yin et al., 2018; Li et al., 2015; Sprengelmeyer et al., 2011) fatigue (Schnellbächer et al., 2021), neurodegenerative diseases such as Alzheimer's disease or frontotemporal dementia (Benarroch, 2019), bipolar disorder and schizophrenia (Li et al., 2018; Takahashi et al., 2020). The prominent role of the insula in such a broad array of diseases underscores its significance both in terms of a reflection of its importance but also as a potential sign of vulnerability. There is a known tendency of neuronal network hubs like the insula, the so-called "rich club" of cortical regions, to be disrupted by various processes (Griffa and Van den Heuvel, 2018). However, how and the extent to which MDD might alter the insular cortex on a structural level remains largely opaque.

High-quality, connectivity-based data acquired by the Human Connectome Project (Van Essen et al., 2012) has enabled the fine-grained segmentation of the insular cortex into six subregions (Fan et al., 2016). These subregions delineate varying patterns of convergence with other cerebral structures, making them separate sub-nodes within the hub region that is the insular cortex. Using 7 Tesla ultra-high field strength structural MRI, our study attempts to analyse alterations in these sub-nodes in patients hospitalized due to MDD. A voxel-by-voxel volume investigation was performed using voxel-based morphometry analysis (VBM) (Ashburner and Friston, 2005). To increase the scope of this investigation, we also examined cortical thickness (Winkler et al., 2010), where prior research found signs of alterations in the insular cortex in case of MDD (Li et al., 2020, Zhao et al., 2017, Zorlu et al., 2017). Cortical thickness was estimated using the projection-based thickness (PBT) method (Dahnke et al., 2013). Additionally, we tested for a possible association of volume and thickness changes with the extent of depressive symptomatology. To our knowledge, this is the first 7 Tesla MRI-based analysis of the insular cortex in depression patients. We hypothesize that employing ultra-high field strength volumetric MRI will allow for a differentiated delineation of significant alterations in MDD patients.

2. Materials and methods

Thirty-three patients suffering from a MDD were recruited at the Universitätsklinik Aachen (mean age = 31.85, standard deviation = 7.97, 16 females). Thirty-one healthy age-matched controls were also recruited (mean age = 28.97, standard deviation = 8.90, 16 females). All participants were between 18 and 50 years of age. Age and gender were not significantly different between groups (age: $p = 0.177$, gender: $p = 0.802$). Eligible patients had a primary diagnosis of MDD, without psychotic features, according to the ICD-10 and DSM-5 criteria. History of concussion or head injury was unknown for the sample. Healthy controls had no current or lifetime psychiatric or neurologic disorder as determined by the SCID-I (First et al., 2002). Handedness was assessed using the Edinburgh Handedness Inventory (Oldfield, 1971). Only right-handed participants were included. All volunteers received compensation for their participation based on the time spent and their travel expenses. Participants with MRI contraindications or unstable medical conditions on the day of the scan were also excluded.

Depressive symptomology and severity were assessed using the Beck Depression Inventory (BDI-II; range 0–63) (Beck et al., 1996) and the AMDP system. The AMDP is an interview-based test, which was developed for the objective monitoring of psychiatric therapy success and is widely used in the German-speaking countries. (Stieglitz et al., 2017). A higher score indicates greater severity of depression in both test systems. AMDP evaluations were performed by trained clinical raters. BDI-II self-assessment and AMDP rating both took place within one week of the MRI scan. All participants gave fully-informed written consent prior to investigation. This protocol was approved by the local Ethics Committee of the Universitätsklinik Aachen. All methods were performed in accordance with the relevant guidelines and regulations.

2.1. MRI acquisition

MRI data acquisition was performed at the Institute of Neuroscience and Medicine-4 (INM-4), Forschungszentrum Jülich using a 7T Magnetom Terra scanner (Siemens Healthineers, Erlangen, Germany) equipped with a 1Tx 32Rx Head Coil 7T Clinical from Nova Medical (Wilmington, MA, USA).

MP2RAGE is a variation of the standard magnetization prepared rapid gradient echo (MPRAGE) sequence. The MP2RAGE acquires two gradient echo images with different inversion time (IT) and flip angle (FA) (inversion image 1 (INV1) IT = 840 ms, flip, FA = 4°, INV2 IT = 2370 ms, FA = 5°). The other sequence related parameters were similar for both gradient echo images Echo time (TE) = 1.99 ms; repetition time (TR) = 4500 ms for signal-to-noise ratio (SNR) optimization. The image matrix was set to 320 × 300 achieving a 0.75 mm isotropic resolution in 208 sagittal slices. The T1 weighted anatomical images referred here were produced by combining the two gradient echo images by means of a ratio as explained by Marques et al. (2010). The combined image was free from proton density contrast, T2* contrast, reception bias field, and first order transmit field inhomogeneity.

2.2. Structural MR data preprocessing

The raw DICOM scans were converted to 3D T1 weighted Neuroimaging Informatics Technology Initiative (NIfTI) format, using MRIcron software (https://www.nitrc.org/projects/mricron). The 3D T1 weighted images were visually audited to check for poor scan quality, artefacts and abnormal tissues using FSL View software (https://fsl.fmrib.ox.ac.uk/fsl/fslwiki/FslView). In the next step, VBM was performed using CAT12.8 (version 1907) (https://www.neuro.uni-jena.de/cat/index.html#VBM) which is designed to work with Statistical Parametric Mapping (SPM12) toolbox (https://www.fil.ion.ucl.ac.uk/spm/software/spm12/) and MATLAB (version 9.7 (R2019b)). VBM preprocessing was performed using CAT12.8 with default settings. The initial voxel based processing included spatial adaptive non-local means (SANLM) denoising filter (Manjón et al., 2010), bias correction, affine registration to improve initial segmentation followed by "unified segmentation" using standard Tissue Probability Map (TPM) provided by the SPM toolbox (Ashburner and Friston, 2005). The results from "unified segmentation" provided the starting estimates for the successive

refined voxel-based processing. In the refined voxel-based processing, further preprocessing steps are performed followed by segmentation and spatial registration to a common reference space. The preprocessing steps in refined voxel-based processing included skull stripping using adaptive probability region-growing (APRG) method, parcellation (into the left and right hemisphere, subcortical areas, and the cerebellum), white matter hyperintensities detection, and local intensity transformation of all tissue classes. These preprocessing steps were followed by an adaptive maximum a posteriori (AMAP) segmentation (Rajapakse et al., 1997) and partial volume estimation for each voxel (Tohka et al., 2004). Finally, the tissue segments are spatially normalized to MNI152NLin2009cAsym reference space using DARTEL (Ashburner, 2007). The GMV within insular sub-regions of interest was calculated using the Brainnetome Atlas (Fan et al., 2016). The Brainnetome Atlas identifies a ventral agranular insula (vla), a ventral dysgranular/granular insula (vld/vlg), a dorsal agranular (dla), dorsal dysgranular (dld), dorsal granular (dlg) and a hypergranular (G) insula for each hemisphere. The mean value of grey matter voxels within the insular subregions was computed for each region of interest in the native space of each subject.

Following the voxel based processing, the surface-based processing steps were performed utilizing CAT12.8 with default settings. Using a PBT method (Dahnke et al., 2013), the cortical thickness estimation and reconstruction of the central surface were completed in a single step. Subsequently, the topological defects were corrected using spherical harmonics (Yotter et al., 2011a) followed by surface refinement which resulted in the final central surface mesh. The individual central surfaces are spatially registered to the 'FsAverage' template of Freesurfer, using a spherical mapping with minimal distortions (Yotter et al., 2011b). Finally, the local thickness values are transferred onto the 'FsAverage' template.

The mean cortical thickness was estimated in the native space of each subject within insular regions using the Destrieux-Atlas (Destrieux et al., 2010). In the Destrieux-Atlas, the insula was segmented bilaterally as the superior (S_circular_insula_sup), anterior (S_circular_insula_ant) and inferior (S_circular_insula_inf) circular sulcus of the insula, the anterior part of the lateral sulcus with its vertical (Lat_Fis-ant-Vertical) and horizontal (Lat_Fis-ant-Horizont) rami, the posterior part of the lateral sulcus (Lat_Fis-post), the short insular gyri (G_insular_short) and the posterior long insular gyri (G_Ins_lg_and_S_cent_ins).

The mean GMV and cortical thickness of insular sub-regions from Brainnetome atlas and the Destrieux-Atlas were considered for further statistical processing respectively.

The segmented images were inspected visually for non-brain structures by overlaying GM segments on the structural image for each subject. Additionally, the CAT toolbox provided automated image and preprocessing quality scores for each subject. Image quality before preprocessing was accessed via weighted overall image quality score accounting for resolution, noise and bias. The mean weighted overall image quality was 90 ± 1.1 % for all subjects. In addition, the quality of the extracted surface was verified via surface Euler number (the number of topology defects) and defect area in percentage. The mean Euler number was 116 ± 57 and the mean defect area was 3.7 ± 2 % for all subjects. These details are added to the manuscript now.

2.3. Statistical analysis

Statistical analysis was performed using SPSS (version 28.0) software package. Demographic and clinical data were analysed using a chi-squared test (for gender) and an independent sample *t*-test (for age) with a significance threshold of $p < 0.05$. Differences in mean GMV and cortical thickness within insular subregions between the MDD patients and healthy control group were analysed using two-tailed ANCOVA. Here the independent variable was group affiliation and the twelve insular subregions were the dependent ones. Adjustments were made for total intracranial volume (TIV), age and gender for GMV. Furthermore, to elucidate the association between BDI-II score and AMDP in MDD with mean GMVs and cortical thickness within insular subregions in MDD patients, linear regression analysis was performed while controlling for age, gender and TIV in case of volumes and age and gender in case of thickness. One patient was excluded from regression analysis due to language difficulties confounding test evaluation. Two other BDI-II test results were excluded since the MDD patients failed to submit the BDI-II in time. Corrections for multiple comparisons were performed using a false-discovery rate (FDR) on the *p*-value outputs, accounting for separate testing of insular subfields. The homogeneity of variance was ensured with Levene's test, and the normal distribution of residues was confirmed with the Shapiro-Wilk test. The significance level was assumed at $p < 0.05$, and the effect size was determined via partial η^2 (Fig. 1).

2.4. Data availability

Data used in this study can be made available through contact with the principal investigator, Prof. Dr. Neuner.

3. Results

3.1. Insular subfields

GMV and cortical thickness of insular subfields in both the left and right hemispheres delineated significant results (before corrections for multiple comparisons), supporting the hypothesis that insular subregions normalized to age and gender differ between groups. However, following corrections for multiple comparisons, significant intergroup differences were seen only in the GMV of ventral left-sided dorsal granular insula ($F(1, 59) = 12.876$, $p_{fdr} = 0.012$, $\eta_p^2 = 0.179$) (Fig. 2, Supplementary Table 3). Cortical thickness analysis within insular regions did not delineate any significant differences between healthy controls and MDD patients after corrections for multiple comparisons (Supplementary Fig. 1, Supplementary Table 3).

3.2. Regression analysis

Regression analyses in the MDD group, adjusted for TIV, age and gender in case of VBM-data and corrected for age and gender in case of cortical thickness measurements, were used to investigate possible associations between structural changes and MDD severity, as quantified by the BDI-II and the AMDP. Regression analyses in the MDD group, demonstrated a strongly significant correlation between AMDP-scores and cortical thickness in the right superior segment of the circular insular sulcus ($\beta = 0.573$, $p_{fdr} = 0.008$). There were no correlations between GMV results and test psychology surviving correction for multiple comparisons with, however, one salient BDI-II correlation in the right ventral agranular insular cortex ($\beta = -0.384$, $p = 0.006$, $p_{fdr} = 0.072$ (Fig. 3).

4. Discussion

Enhanced signal 7 *T*-MRI subfield analysis confirmed a significant influence of MDD on GMV in the dorsal granular part of the left insular cortex. Cortical thickness positively correlated with disease severity in the right superior segment of the circular insular sulcus. Our results emphasize the role of the insula in the pathogeneses of depression and allow for deductive reasoning regarding pathophysiology in the context of "rich club" vulnerability.

The insula is divided into an anterior and a posterior lobule by a central sulcus. The posterior lobule of the insula generally is segmented into two long gyri, while the anterior lobule usually contains three short gyri with an additional accessory gyrus situated more ventrally (Benarroch, 2019). The anterior-to-posterior axis is marked by an intensifying degree of granulation. The Brainnetome nomenclature

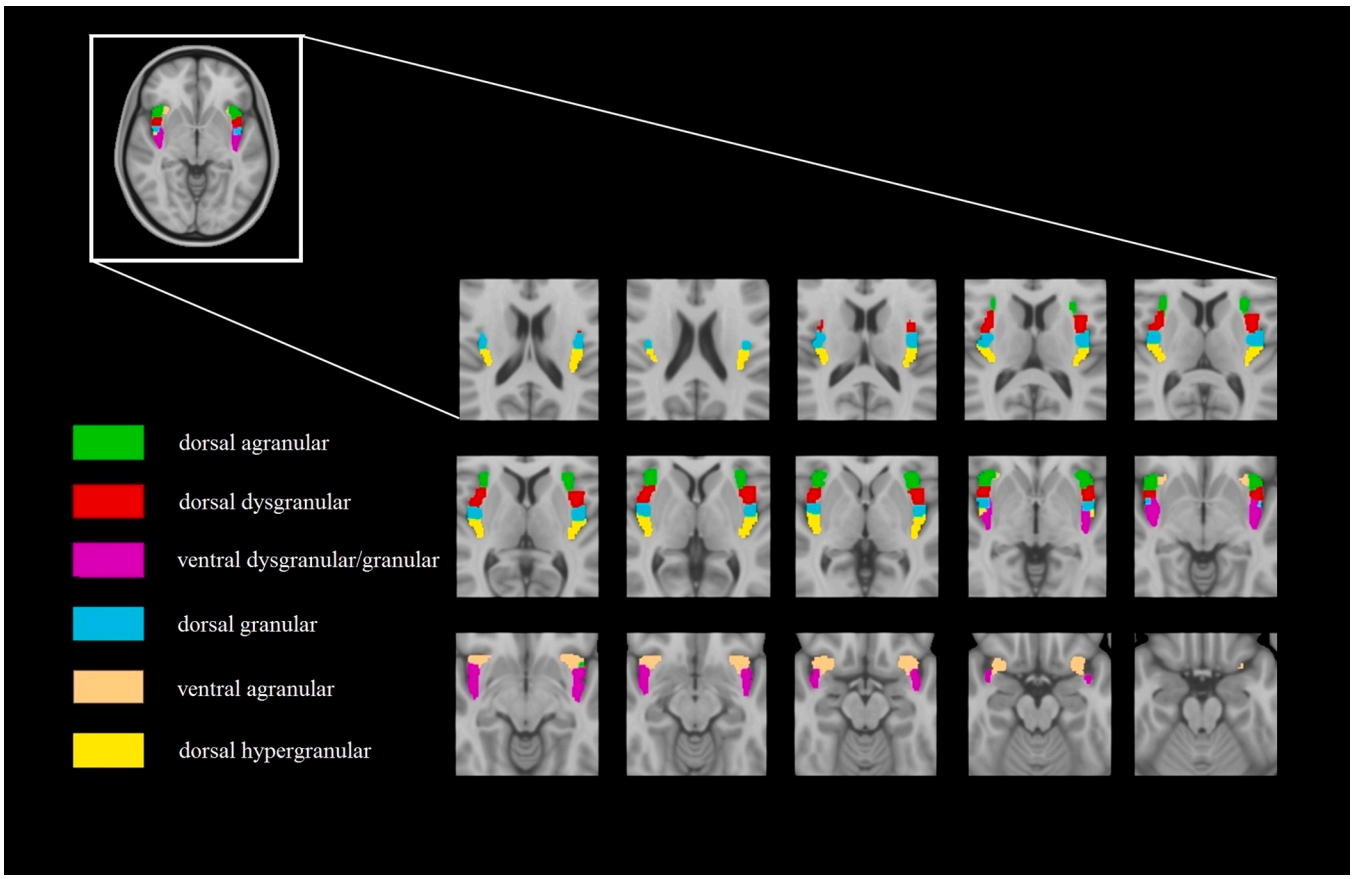

Fig. 1. Structural representation of insular subfield extensions according to the Brainnetome atlas. Significant intergroup differences were found in the left dorsal granular insula.

omits the anterior-to-posterior parcellation in favour of a description based on granulation levels in combination with spatial information along a ventral-to-dorsal axis. Fig. 2 demonstrates that this system corresponds with the known anterior vs posterior dichotomy. Noting this, our results can be embedded into existing scientific research. The anterior insula has long been identified as a vital part of the salience network (Uddin, 2015; Seeley et al., 2007; Benarroch, 2019). The insula contributes to a dorsal frontoparietal, bottom-up, stimulus-driven network directing attention (Uddin, 2015) and the right insular cortex is particularly involved in the switch between the externally directed central executive network and the internally directed default-mode network (Uddin et al., 2011; Sridharan et al., 2008). Inter-network switches, such as this one, have been shown to be compromised in the case of post-traumatic stress disorder and depression (Daniels et al., 2010; Zheng et al., 2015). The insula might also prioritize which information is being processed and introduced into the global neuronal workspace (Michel, 2017). In order to fulfil such roles, it is necessary to combine external and internal input to acquire an accurate picture of the current state of the organism as a whole. Only through the representation of multimodal content can a basis of information sufficient to complete such complex and directive functions be achieved.

Multimodal integration is based on several functional axes underlying intra-insular connectivity (Evrard, 2019). The sensory-motor axis is reminiscent of the dichotomy between the granular primary sensory area and the agranular motor cortex. The posterior granular insula is the main entry point for detailed sensory information from, for instance, the nucleus of the solitary tract, the superior temporal cortex or the auditory cortex (Craig, 2014; Deen et al., 2011), while the agranular anterior cortex contains with the von Economo-neurons specialized projecting cells (Carmichael and Price, 1995), similar to the motor cortex, and its Betz cells (Craig, 2006). Another axis describes the processing of autonomous nervous system information in the insular cortex, namely the interplay of sympathetic and parasympathetic connections. The ascending sympathetic fibres seem to focus on the posterior insula, while the parasympathetic ones are more prominent in the anterior insula (Keizer and Kuypers, 1984). Both granular and dysgranular parts differentiate in an inter-personal/ventral part and an intra-personal/dorsal one. While the dorsal dysgranular area receives a somatotopic input from i.e. the primary sensory area, the ventral dysgranular one is connected to structures like the ventral striatum, anterior cingulate cortex and amygdala associated with emotional regulation (Cardinal et al., 2002; DelDonno et al., 2017; Andrewes and Jenkins, 2019). Finally, the anterior agranular insula also has a ventral/dorsal dichotomy, with the ventral part being more involved with emotional processes and the dorsal one with cognitive ones (Kurth et al., 2010a; Kurth et al., 2010b; Chang et al., 2013). These axes of data processing intertwine in a dynamic interplay, leading to a highly complex and sophisticated connectivity architecture (Sridharan et al., 2008). In the anterior insular cortex bottom-up sensory signals combine with top-down higher-order evaluations, possibly leading to a state of awareness (Gu et al., 2013). There seems to be an increasing level of input integration from the granular posterior to the agranular anterior insula.

Our study delineated GMV alterations within the posteriorly located left dorsal granular insula, which receives sensory input sent from i.e. the vegetative nerve system. This is not surprising since depressed mood is heavily influenced by the way a person perceives his or her environment and their own body. Posterior insula alterations in patients suffering from depression or somatoform pain disorder have been previously identified (Soriano-Mas et al., 2011; Meyer et al., 2020). Intra-group regression analysis showed a correlation between disease

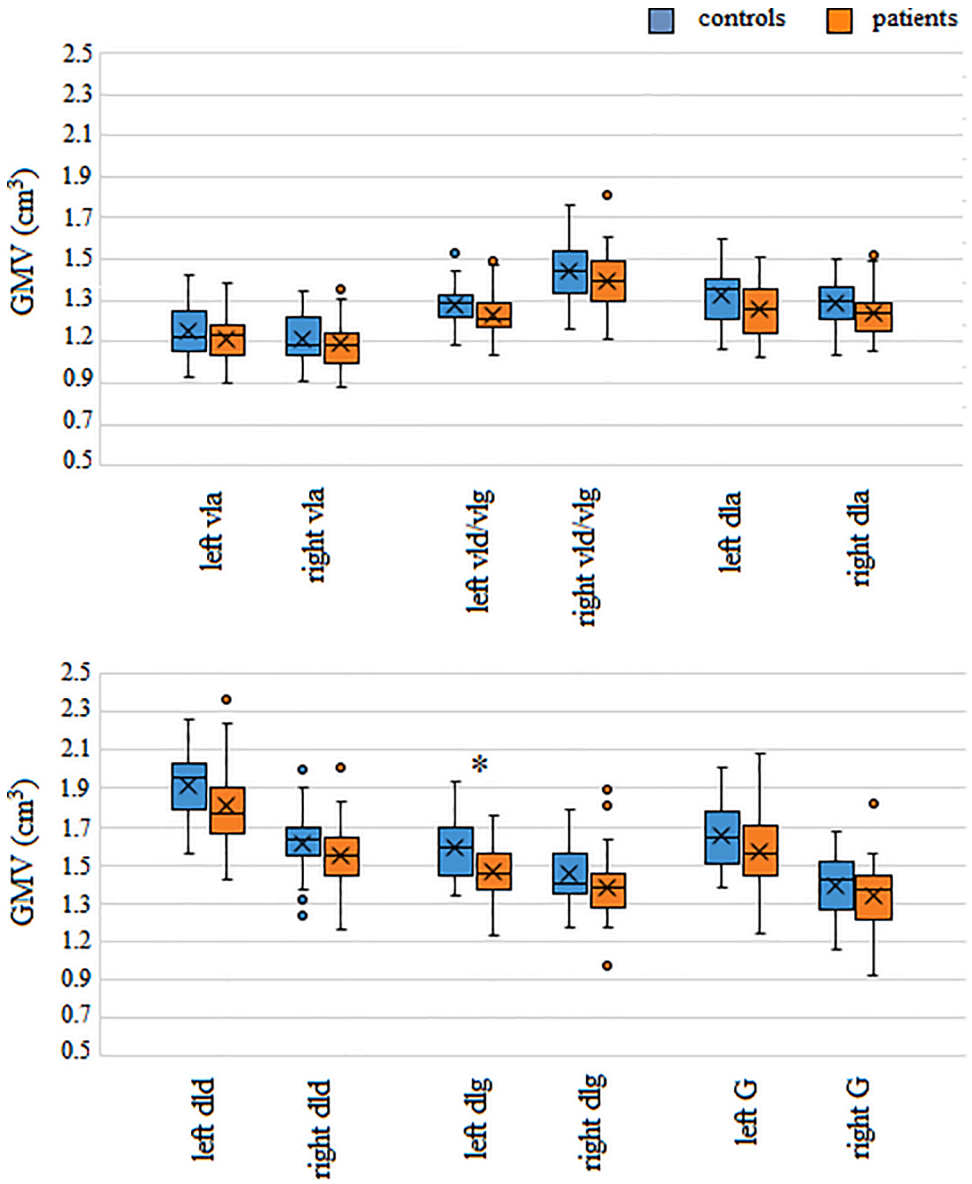

Fig. 2. Boxplots comparing insular subfield volumes of healthy controls with patients. vla: ventral agranular insula; vld/vlg ventral dysgranular and granular insula; dla dorsal agranular insula; dld: dorsal dysgranular insula; dlg: dorsal granular insula; G: dorsal hypergranular insula.

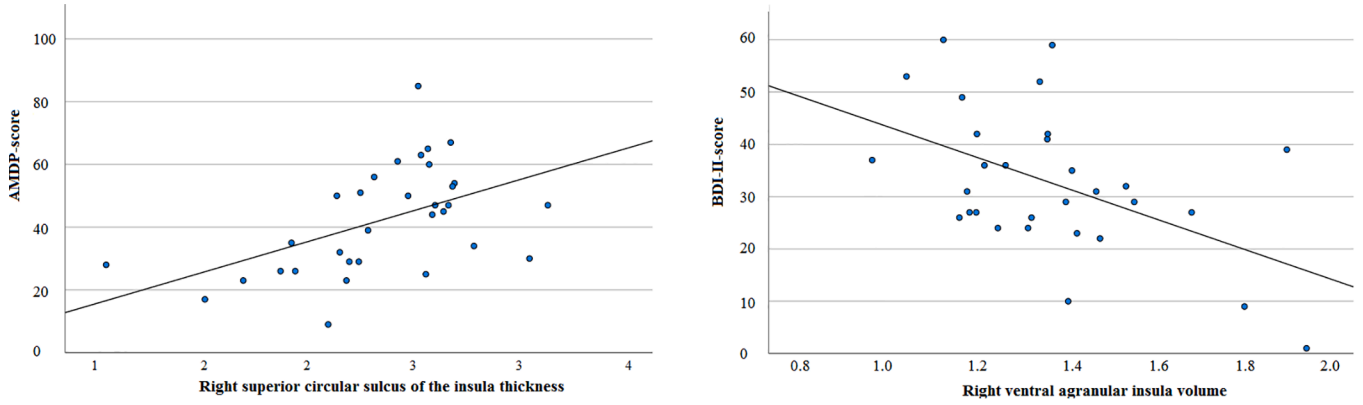

Fig. 3. Scatter plots describing symptom severity correlation (plots do not contain covariates). (**A**) AMDP-score and right superior circular sulcus of the insular thickness ($p_{fdr} = 0.008$). (**B**) BDI-II-score and right ventral agranular insula volume ($p_{fdr} = 0.072$).

severity and cortical thickness in the insular cortex situated under to the superior part of the circular sulcus of the insula that separates this structure from the inferior frontal cortex. There were also signs that grey matter volume negatively correlated with BDI-II scores in the right ventral agranular insula, although these correlations did not survive correction for multiple comparisons (Fig. 3). Fittingly, these more anterior regions play a role in cognition and emotion as described above.

Our results are very much in line with previous research and offer an improved, fine-grained description of insula structure disruption. Their significance is emphasized by the fact that a similar study investigating hippocampal and amygdala subfields in depression patients did not find intergroup differences in GMV (Brown et al., 2019). Furthermore, the results harmonize well with the observation by Drysdale et al. (2017) that the insular cortex is involved in all biotypes of depression. Since in recruitment we did not differentiate between the various patterns of symptomatology i.e. a predominance in anxiety or psychomotor retardation, it seems reasonable to assume that the ubiquity of insular affection in MDD was a contributing factor to statistical significance.

This leads to the question of the reason for the morphological changes of the left insula. Disruptions of the connectome are a general feature of both neurological and psychiatric diseases (de Lange et al., 2019). The insula is a prominent node of the cerebral connectome and part of the "rich club" of highly connected regions (Bassett et al., 2008; Harriger et al., 2012). These hubs tend to be vulnerable to pathological processes (Van Essen et al., 2012; Dai et al., 2015). Central network positions correlate with a higher burden of lesions in both grey and white matter, in contrast to less affected areas in the periphery (Crossley et al., 2014, Klauser et al., 2017; Griffa et al., 2013). Several factors, such as increased metabolism, network spreading or genetics (Van Essen et al., 2012; Buckholtz and Meyer-Lindenberg, 2012) are known to contribute to this circumstance. "Rich club" organization offers computational benefits but can also be locally cost-intensive. Metabolic turn-over might lead to an accumulation of by-products of aerobic glycolysis compromising structural integrity (Van Essen et al., 2012). High levels of microstructural organization and myelination associated with "rich club" characteristics (Collin et al., 2014) may augment the impact of such processes. It seems intuitive that regions with high levels of both complexity and activity, as seen in the insular cortex, are the first affected in the case of neuronal strain. A lack of the antioxidant glutathione has been associated with connectome disruptions and the development of schizophrenia (Collin et al., 2017) suggesting "rich club" vulnerability to free radicals. Hypothalamic-pituitary-adrenal axis hyperactivity and inflammation correlate with depressive symptomatology in rats (Becker et al., 2008) as well as humans and seems most prominent in case of somatic symptoms in comparison to cognitive-affective ones (Iob et al., 2020). Cortical thickness positively correlated with disease severity around the superior circular sulcus suggesting a MDD related dynamic process of microstructural reorganization possibly caused by metabolic factors.

Another possible reason for GMV reduction may be found in the insula's extensive functional convergence across the brain. Pathological processes may transmit via axonal routes leading to disruption patterns not defined by spatial proximity but rather by connectivity (Warren et al., 2012). Considering that network spreading is associated with proteinopathies (Warren et al., 2013), as found, for example, in cognitive decline (Schnellbächer et al., 2020) occurrence in our relatively young patient population is unlikely. However, it seems plausible that neurodegenerative processes may lead to depressive symptoms via network spreading. A kinetic model simulating the spread of Alzheimer's disease delineated that the dynamic was fastest if it was centred in the insula and the putamen (Fornari et al., 2019). Additionally, the position of the insula within the central autonomic network (Benarroch, 1993; Wei et al., 2018) could make it susceptible to synoclueinopathies like Parkinson's disease. Enterally resorbed proteins may travel along vagal fibres to the brain, eventually reaching the insular cortex (Braak and Del Tredici, 2008). Thus, while network spreading most likely did not significantly influence our results due to the relatively young patient population used in this study, the insular cortex as a network hub seems vulnerable to such pathology.

A prior investigation demonstrated structural changes in the left anterior insula in both patients with current and remitted depressive disease in comparison to healthy controls (Li et al., 2015). The authors interpreted anterior insula morphologic abnormalities as a biological marker of vulnerability. Similarly, our results demonstrated a reduced GMV in the left dorsal granular insula in patients that did not correlate with disease severity. This could be a sign of factors independent from disease course, leading to the question of how far genetics contribute to insular disruption. Generally, there is a clear association between MDD and heritable factors. A twin study demonstrated how heritability of tendency to develop depression is around 29 % for males and 42 % for females (Kendler et al., 2006). While no clear principle of generational risk transmission has been identified to date, there have been several indications that genes influence depressive symptomatology. In the specific case of the insula, it could be shown that genetic alterations of insular *N*-methyl-D-aspartate (NMDA)-receptors in mice influence pain perception (Wei et al., 2001). The insular cortex exhibits an enriched expression of genes associated with mood disorders, learning, and glutamate and dopamine signalling (Ibrahim et al., 2019). However, in a structural connectivity analysis of single nucleotid polymorphisms in a pediatric population, the insular cortex was not found to feature prominently (Taquet et al., 2021). Clearly, the influence of genetic risk factors on insular cortex affection remains remarkably opaque, and future studies are required to clarify this circumstance.

Limiting interpretability of our results is a modest effect strength, meaning that only parts of variation can be explained by our model. This indicates that the delineated data may allow for interpretation regarding pathophysiology, but the predictive power of insular structural alterations in the case of MDD is low. Their usage for diagnostic purposes may only be prudent as a variable of a multivariate analysis and not in isolation. The low effect size, however, also underscores the importance of ultra-high resolution imaging since it is expected that results would have been less significant if a lower magnetic field strength had been used.

In conclusion, there is a GMV reduction in the granular regions of the left insular cortex in MDD patients in comparison to healthy, matched controls. Cortical thickness in the superior circular sulcus positively correlates with disease severity. The insula cortex as a highly connected hub regions seems vulnerable to various forms of disruption.

Funding

No funding was received for this work.

CRediT authorship contribution statement

Gereon J. Schnellbächer: Conceptualization, Formal analysis, Writing – original draft, Writing – review & editing. **Ravichandran Rajkumar:** Conceptualization, Methodology. **Tanja Veselinović:** Project administration. **Shukti Ramkiran:** Software, Data curation. **Jana Hagen:** Data curation, Formal analysis. **N. Jon Shah:** Supervision. **Irene Neuner:** Supervision.

Declaration of Competing Interest

The authors declare that they have no known competing financial interests or personal relationships that could have appeared to influence the work reported in this paper.

Data availability

Data will be made available on request.

Appendix A. Supplementary data

Supplementary data to this article can be found online at https://doi.org/10.1016/j.nicl.2022.103249.

References

Almashaikhi, T., Rheims, S., Ostrowsky-Coste, K., Montavont, A., Jung, J., De Bellescize, J., Arzimanoglou, A., Keo Kosal, P., Guénot, M., Bertrand, O., Ryvlin, P., 2014. Intrainsular functional connectivity in human. Hum. Brain Mapp. 35 (6), 2779–2788.

Andrewes, D.G., Jenkins, L.M., 2019. The role of the amygdala and the ventromedial prefrontal cortex in emotional regulation: implications for post-traumatic stress disorder. Neuropsychol. Rev. 29 (2), 220–243. https://doi.org/10.1007/s11065-019-09398-4.

Ashburner, J., 2007. A fast diffeomorphic image registration algorithm. NeuroImage 38 (1), 95–113. https://doi.org/10.1016/j.neuroimage.2007.07.007.

Ashburner, J., Friston, K.J., 2005. Unified segmentation. NeuroImage 26 (3), 839–851. https://doi.org/10.1016/j.neuroimage.2005.02.018.

Bassett, D.S., Bullmore, E., Verchinski, B.A., Mattay, V.S., Weinberger, D.R., Meyer-Lindenberg, A., 2008. Hierarchical organization of human cortical networks in health and schizophrenia. J. Neurosci. 28 (37), 9239–9248.

Beck, A.T., Steer, R.A.., Brown, G.K. 1996. Beck depression inventory (BDI-II). Pearson.; 10: s15327752jpa6703_13.

Becker, C., Zeau, B., Rivat, C., Blugeot, A., Hamon, M., Benoliel, J.-J., 2008. Repeated social defeat-induced depression-like behavioral and biological alterations in rats: involvement of cholecystokinin. Mol. Psychiatry 13 (12), 1079–1092.

Benarroch, E.E., 1993. The central autonomic network: functional organization, dysfunction, and perspective. Mayo Clin. Proc. 68 (10), 988–1001. https://doi.org/10.1016/s0025-6196(12)62272-1.

Benarroch, E.E., 2019. Insular cortex: Functional complexity and clinical correlations. Neurology 93 (21), 932–938. https://doi.org/10.1212/WNL.0000000000008525.

Braak, H., Del Tredici, K., 2008. Invited Article: Nervous system pathology in sporadic Parkinson disease. Neurology 70 (20), 1916–1925. https://doi.org/10.1212/01.wnl.0000312279.49272.9f.

Brown, S.S.G., Rutland, J.W., Verma, G., Feldman, R.E., Alper, J., Schneider, M., Delman, B.N., Murrough, J.M., Balchandani, P., 2019. Structural MRI at 7T reveals amygdala nuclei and hippocampal subfield volumetric association with Major Depressive Disorder symptom severity. Sci. Rep. 9 (1) https://doi.org/10.1038/s41598-019-46687-7.

Buckholtz, J.W., Meyer-Lindenberg, A., 2012. Psychopathology and the human connectome: toward a transdiagnostic model of risk for mental illness. Neuron 74 (6), 990–1004. https://doi.org/10.1016/j.neuron.2012.06.002.

Cardinal, R.N., Parkinson, J.A., Hall, J., Everitt, B.J., 2002. Emotion and motivation: the role of the amygdala, ventral striatum, and prefrontal cortex. Neurosci. Biobehav. Rev. 26 (3), 321–352.

Carmichael, S.T., Price, J.L., 1995. Limbic connections of the orbital and medial prefrontal cortex in macaque monkeys. J. Comp. Neurol. 363 (4), 615–641. https://doi.org/10.1002/cne.903630408.

Chang, L.J., Yarkoni, T., Khaw, M.W., Sanfey, A.G., 2013. Decoding the role of the insula in human cognition: functional parcellation and large-scale reverse inference. Cereb. Cortex 23 (3), 739–749.

Collin, G., Sporns, O., Mandl, R.C.W., van den Heuvel, M.P., 2014. Structural and functional aspects relating to cost and benefit of rich club organization in the human cerebral cortex. Cereb. Cortex 24 (9), 2258–2267.

Collin, G., Scholtens, L.H., Kahn, R.S., Hillegers, M.H.J., van den Heuvel, M.P., 2017. Affected anatomical rich club and structural-functional coupling in young offspring of schizophrenia and bipolar disorder patients. Biol. Psychiatry 82 (10), 746–755.

Craig, A.D., 2006. Retrograde analyses of spinothalamic projections in the macaque monkey: input to ventral posterior nuclei. J. Comp. Neurol. 499 (6), 965–978. https://doi.org/10.1002/cne.21154.

Craig, A.D., 2014. Topographically organized projection to posterior insular cortex from the posterior portion of the ventral medial nucleus in the long-tailed macaque monkey. J. Comp. Neurol. 522 (1), 36–63. https://doi.org/10.1002/cne.23425.

Crossley, N.A., Mechelli, A., Scott, J., Carletti, F., Fox, P.T., McGuire, P., et al., 2014. The hubs of the human connectome are generally implicated in the anatomy of brain disorders. Brain: J. Neurol. 137 (Pt 8), 2382–2395. https://doi.org/10.1093/brain/awu132.

Dahnke, R., Yotter, R.A., Gaser, C., 2013. Cortical thickness and central surface estimation. NeuroImage 65, 336–348. https://doi.org/10.1016/j.neuroimage.2012.09.050.

Dai, Z.J., Bi, Y.C., He, Y., 2015. With great brain hub connectivity comes great vulnerability. CNS Neurosci. Ther. 21 (7), 541–542. https://doi.org/10.1111/cns.12407.

Daniels, J.K., McFarlane, A.C., Bluhm, R.L., Moores, K.A., Clark, C.R., Shaw, M.E., Williamson, P.C., Densmore, M., Lanius, R.A., 2010. Switching between executive and default mode networks in posttraumatic stress disorder: alterations in functional connectivity. J. Psychiatry Neurosci.: JPN 35 (4), 258–266.

de Lange, S.C., Scholtens, L.H., van den Berg, L.H., Boks, M.P., Bozzali, M., Cahn, W., Dannlowski, U., Durston, S., Geuze, E., van Haren, N.E.M., Hillegers, M.H.J., Koch, K., Jurado, M.Á., Mancini, M., Marqués-Iturria, I., Meinert, S., Ophoff, R.A., Reess, T.J., Repple, J., Kahn, R.S., van den Heuvel, M.P., 2019. Shared vulnerability for connectome alterations across psychiatric and neurological brain disorders. Nat. Hum. Behav. 3 (9), 988–998.

Deen, B., Pitskel, N. B., and Pelphrey, K. A., 2011. Three systems of insular functional connectivity identified with cluster analysis. Cerebral cortex (New York, N.Y. : 1991), 21(7), 1498–1506. https://doi.org/10.1093/cercor/bhq186.

DelDonno, S.R., Jenkins, L.M., Crane, N.A., Nusslock, R., Ryan, K.A., Shankman, S.A., Phan, K.L., Langenecker, S.A., 2017. Affective traits and history of depression are related to ventral striatum connectivity. J. Affect. Disord. 221, 72–80.

Destrieux, C., Fischl, B., Dale, A., Halgren, E., 2010. Automatic parcellation of human cortical gyri and sulci using standard anatomical nomenclature. Neuroimage 53 (1), 1–15.

Drysdale, A.T., Grosenick, L., Downar, J., Dunlop, K., Mansouri, F., Meng, Y., Fetcho, R. N., Zebley, B., Oathes, D.J., Etkin, A., Schatzberg, A.F., Sudheimer, K., Keller, J., Mayberg, H.S., Gunning, F.M., Alexopoulos, G.S., Fox, M.D., Pascual-Leone, A., Voss, H.U., Casey, B.J., Dubin, M.J., Liston, C., 2017. Resting-state connectivity biomarkers define neurophysiological subtypes of depression. Nat. Med. 23 (1), 28–38.

Evrard, H.C., 2019. The organization of the primate insular cortex. Front. Neuroanat. 13, 43. https://doi.org/10.3389/fnana.2019.00043.

Fan, L., Li, H., Zhuo, J., Zhang, Y.u., Wang, J., Chen, L., Yang, Z., Chu, C., Xie, S., Laird, A.R., Fox, P.T., Eickhoff, S.B., Yu, C., Jiang, T., 2016. The human brainnetome atlas: a new brain atlas based on connectional architecture. Cereb. Cortex 26 (8), 3508–3526.

First, M.B., Spitzer, R.L., Gibbon, M., Williams, J.B.W., 2002. Structured clinical interview for DSM-IV-TR axis I disorders, research version, patient edition. (SCID-I/P). *New York: Biometrics Research.*;New York State Psychiatric Institute..

Fornari, S., Schäfer, A., Jucker, M., Goriely, A., Kuhl, E., 2019. Prion-like spreading of Alzheimer's disease within the brain's connectome. J. R. Soc. Interface 16 (159), 20190356.

Friedrich, M.J., 2017. Depression is the leading cause of disability around the world. JAMA 317 (15), 1517. https://doi.org/10.1001/jama.2017.3826:1517.

Gogolla, N., 2017. The insular cortex. Current Biol.: CB 27 (12), R580–R586.

Griffa, A., Baumann, P.S., Thiran, J.-P., Hagmann, P., 2013. Structural connectomics in brain diseases. NeuroImage 80, 515–526.

Griffa, A., Van den Heuvel, M.P., 2018. Rich-club neurocircuitry: function, evolution, and vulnerability. Dialogues Clinical Neurosci. 20 (2), 121–132. https://doi.org/10.31887/DCNS.2018.20.2/agriffa.

Gu, X., Hof, P.R., Friston, K.J., Fan, J., 2013. Anterior insular cortex and emotional awareness. J. Comp. Neurol. 521 (15), 3371–3388.

Harriger, L., van den Heuvel, M.P., Sporns, O., Kaiser, M., 2012. Rich club organization of macaque cerebral cortex and its role in network communication. PLoS ONE 7 (9), e46497.

Ibrahim, C., Le Foll, B., French, L., 2019. Transcriptomic characterization of the human insular cortex and claustrum. Front. Neuroanat. 13, 94. https://doi.org/10.3389/fnana.2019.00094.

Iob, E., Kirschbaum, C., Steptoe, A., 2020. Persistent depressive symptoms, HPA-axis hyperactivity, and inflammation: the role of cognitive-affective and somatic symptoms. Mol. Psychiatry 25 (5), 1130–1140. https://doi.org/10.1038/s41380-019-0501-6.

Keizer, K., Kuypers, H.G., 1984. Distribution of corticospinal neurons with collaterals to lower brain stem reticular formation in cat. Exp. Brain Res. 54 (1), 107–120. https://doi.org/10.1007/BF00235823.

Kendler, K.S., Gatz, M., Gardner, C.O., Pedersen, N.L., 2006. A Swedish national twin study of lifetime major depression. Am. J. Psychiatry 163 (1), 109–114.

Klauser, P., Baker, S. T., Cropley, V. L., Bousman, C., Fornito, A., Cocchi, L., et al., 2017. White Matter Disruptions in Schizophrenia Are Spatially Widespread and Topologically Converge on Brain Network Hubs. Schizophrenia Bull., 43(2), 425–435. https://doi.org/10.1093/schbul/sbw100.

Kurth, F., Zilles, K., Fox, P.T., Laird, A.R., Eickhoff, S.B., 2010a. A link between the systems: functional differentiation and integration within the human insula revealed by meta-analysis. Brain Struct. Funct. 214 (5-6), 519–534.

Kurth, F., Eickhoff, S.B., Schleicher, A., Hoemke, L., Zilles, K., Amunts, K., 2010b. Cytoarchitecture and probabilistic maps of the human posterior insular cortex. Cereb. Cortex 20 (6), 1448–1461.

Li, W., Douglas Ward, B., Liu, X., Chen, G., Jones, J.L., Antuono, P.G., Li, S.-J., Goveas, J. S., 2015. Disrupted small world topology and modular organisation of functional networks in late-life depression with and without amnestic mild cognitive impairment. J. Neurol. Neurosurg. Psychiatry 86 (10), 1097–1105.

Li, J., Tang, Y., Womer, F., Fan, G., Zhou, Q., Sun, W., Xu, K.e., Wang, F., 2018. Two patterns of anterior insular cortex functional connectivity in bipolar disorder and schizophrenia. World J. Biol. Psychiatry 19 (sup3), S115–S123.

Li, Q., Zhao, Y., Chen, Z., Long, J., Dai, J., Huang, X., Lui, S.u., Radua, J., Vieta, E., Kemp, G.J., Sweeney, J.A., Li, F., Gong, Q., 2020. Meta-analysis of cortical thickness abnormalities in medication-free patients with major depressive disorder. Neuropsychopharmacology 45 (4), 703–712.

Manjón, J.V., Coupé, P., Martí-Bonmatí, L., Collins, D.L., Robles, M., 2010. Adaptive non-local means denoising of MR images with spatially varying noise levels. J. Magnetic Resonance Imag. : JMRI 31 (1), 192–203. https://doi.org/10.1002/jmri.22003.

Marques, J.P., Kober, T., Krueger, G., et al., 2010. MP2RAGE, a self bias-field corrected sequence for improved segmentation and T1-mapping at high field. NeuroImage 49 (2), 1271–1281.

Mesulam, M.M., Mufson, E.J., 1982. Insula of the old world monkey. I. Architectonics in the insulo-orbito-temporal component of the paralimbic brain. J. Comp. Neurol. 212 (1), 1–22. https://doi.org/10.1002/cne.902120102.

Meyer, E., Morawa, E., Nacak, Y., Rösch, J., Doerfler, A., Forster, C., et al., 2020. Insular cortical thickness in patients with somatoform pain disorder: are there associations with symptom severity and childhood trauma? Front. Psychiatry 11, 497100. https://doi.org/10.3389/fpsyt.2020.497100.

Michel, M., 2017. A role for the anterior insular cortex in the global neuronal workspace model of consciousness. Conscious. Cogn. 49, 333–346. https://doi.org/10.1016/j.concog.2017.02.004.
Oldfield, R.C., 1971. The assessment and analysis of handedness: the Edinburgh inventory. Neuropsychologia 9 (1), 97–113. https://doi.org/10.1016/0028-3932(71)90067-4.
Rajapakse, J.C., Giedd, J.N., Rapoport, J.L., 1997. Statistical approach to segmentation of single-channel cerebral MR images. IEEE Trans. Med. Imaging 16 (2), 176–186. https://doi.org/10.1109/42.563663.
Schnellbächer, G.J., Hoffstaedter, F., Eickhoff, S.B., Caspers, S., Nickl-Jockschat, T., Fox, P.T., Laird, A.R., Schulz, J.B., Reetz, K., Dogan, I., 2020. Functional characterization of atrophy patterns related to cognitive impairment. Front. Neurol. 11 https://doi.org/10.3389/fneur.2020.00018.
Schnellbächer, G.J., Kettenbach, S., Löffler, L., Dreher, M., Habel, U., Votinov, M., 2021. Morphological profiles of fatigue in Sarcoidosis patients. Psychiatry Res. Neuroimag. 315, 111325.
Seeley, W.W., Menon, V., Schatzberg, A.F., Keller, J., Glover, G.H., Kenna, H., Reiss, A.L., Greicius, M.D., 2007. Dissociable intrinsic connectivity networks for salience processing and executive control. J. Neurosci. 27 (9), 2349–2356.
Soriano-Mas, C., Hernández-Ribas, R., Pujol, J., Urretavizcaya, M., Deus, J., Harrison, B. J., Ortiz, H., López-Solà, M., Menchón, J.M., Cardoner, N., 2011. Cross-sectional and longitudinal assessment of structural brain alterations in melancholic depression. Biol. Psychiatry 69 (4), 318–325.
Sprengelmeyer, R., Steele, J.D., Mwangi, B., Kumar, P., Christmas, D., Milders, M., Matthews, K., 2011. The insular cortex and the neuroanatomy of major depression. J. Affect. Disord. 133 (1-2), 120–127.
Sridharan, D., Levitin, D.J., Menon, V., 2008. A critical role for the right fronto-insular cortex in switching between central-executive and default-mode networks. PNAS 105 (34), 12569–12574.
Stieglitz, R.-D., Haug, A., Fähndrich, E., Rösler, M., Trabert, W., 2017. Comprehensive psychopathological assessment based on the association for methodology and documentation in psychiatry (AMDP) system: development, methodological foundation, application in clinical routine, and research. Front. Psychiatry 8. https://doi.org/10.3389/fpsyt.2017.00045.
Takahashi, T., Yücel, M., Lorenzetti, V., Tanino, R., Whittle, S., Suzuki, M., Walterfang, M., Pantelis, C., Allen, N.B., 2010. Volumetric MRI study of the insular cortex in individuals with current and past major depression. J. Affect. Disord. 121 (3), 231–238.
Takahashi, T., Kido, M., Sasabayashi, D., Nakamura, M., Furuichi, A., Takayanagi, Y., Noguchi, K., Suzuki, M., 2020. Gray matter changes in the insular cortex during the course of the schizophrenia spectrum. Front. Psychiatry 11. https://doi.org/10.3389/fpsyt.2020.00659.
Taquet, M., Smith, S.M., Prohl, A.K., Peters, J.M., Warfield, S.K., Scherrer, B., Harrison, P.J., 2021. A structural brain network of genetic vulnerability to psychiatric illness. Mol. Psychiatry 26 (6), 2089–2100.
Tohka, J., Zijdenbos, A., Evans, A., 2004. Fast and robust parameter estimation for statistical partial volume models in brain MRI. NeuroImage 23 (1), 84–97. https://doi.org/10.1016/j.neuroimage.2004.05.007.
Uddin, L.Q., 2015. Salience processing and insular cortical function and dysfunction. Nat. Rev. Neurosci. 16 (1), 55–61. https://doi.org/10.1038/nrn3857.
Uddin, L.Q., Supekar, K.S., Ryali, S., Menon, V., 2011. Dynamic reconfiguration of structural and functional connectivity across core neurocognitive brain networks with development. J. Neurosci. 31 (50), 18578–18589.
Uddin, L.Q., Kinnison, J., Pessoa, L., et al., 2014. Beyond the tripartite cognition-emotion-interoception model of the human insular cortex. J. Cognit. Neurosci. 26 (1), 16–27. https://doi.org/10.1162/jocn_a_00462.
Van Essen, D.C., Ugurbil, K., Auerbach, E., Barch, D., Behrens, T.E.J., Bucholz, R., Chang, A., Chen, L., Corbetta, M., Curtiss, S.W., Della Penna, S., Feinberg, D., Glasser, M.F., Harel, N., Heath, A.C., Larson-Prior, L., Marcus, D., Michalareas, G., Moeller, S., Oostenveld, R., Petersen, S.E., Prior, F., Schlaggar, B.L., Smith, S.M., Snyder, A.Z., Xu, J., Yacoub, E., 2012. The Human Connectome Project: A data acquisition perspective. NeuroImage 62 (4), 2222–2231.
Warren, J.D., Rohrer, J.D., Hardy, J., 2012. Disintegrating brain networks: from syndromes to molecular nexopathies. Neuron 73 (6), 1060–1062. https://doi.org/10.1016/j.neuron.2012.03.006.
Warren, J.D., Rohrer, J.D., Schott, J.M., Fox, N.C., Hardy, J., Rossor, M.N., 2013. Molecular nexopathies: a new paradigm of neurodegenerative disease. Trends Neurosci. 36 (10), 561–569.
Wei, L., Chen, H., Wu, G.R., 2018. Heart rate variability associated with grey matter volumes in striatal and limbic structures of the central autonomic network. Brain Res. 1681, 14–20. https://doi.org/10.1016/j.brainres.2017.12.024.
Wei, F., Wang, G.-D., Kerchner, G.A., Kim, S.J., Xu, H.-M., Chen, Z.-F., Zhuo, M., 2001. Genetic enhancement of inflammatory pain by forebrain NR2B overexpression. Nat. Neurosci. 4 (2), 164–169.
Winkler, A.M., Kochunov, P., Blangero, J., Almasy, L., Zilles, K., Fox, P.T., Duggirala, R., Glahn, D.C., 2010. Cortical thickness or grey matter volume? The importance of selecting the phenotype for imaging genetics studies. NeuroImage 53 (3), 1135–1146.
Yin, Z., Chang, M., Wei, S., Jiang, X., Zhou, Y., Cui, L., Lv, J., Wang, F., Tang, Y., 2018. Decreased functional connectivity in insular subregions in depressive episodes of bipolar disorder and major depressive disorder. Front. Neurosci. 12 https://doi.org/10.3389/fnins.2018.00842.
Yotter, R.A., Dahnke, R., Thompson, P.M., Gaser, C., 2011a. Topological correction of brain surface meshes using spherical harmonics. Hum. Brain Mapp. 32 (7), 1109–1124. https://doi.org/10.1002/hbm.21095.
Yotter, R.A., Nenadic, I., Ziegler, G., Thompson, P.M., Gaser, C., 2011b. Local cortical surface complexity maps from spherical harmonic reconstructions. NeuroImage 56 (3), 961–973. https://doi.org/10.1016/j.neuroimage.2011.02.007.
Zhao, Y., Chen, L., Zhang, W., Xiao, Y., Shah, C., Zhu, H., et al., 2017. Grey matter abnormalities in non-comorbid medication-naive patients with major depressive disorder or social anxiety disorder. EBioMedicine 21, 228–235. https://doi.org/10.1016/j.ebiom.2017.06.013.
Zheng, H., Xu, L., Xie, F., Guo, X., Zhang, J., Yao, L.i., Wu, X., 2015. The altered triple networks interaction in depression under resting state based on graph theory. Biomed Res. Int. 2015, 1–8.
Zorlu, N., Cropley, V.L., Zorlu, P.K., Delibas, D.H., Adibelli, Z.H., Baskin, E.P., Esen, Ö.S., Bora, E., Pantelis, C., 2017. Effects of cigarette smoking on cortical thickness in major depressive disorder. J. Psychiatr. Res. 84, 1–8.